JTTEE5 11:62-68

Finite Element Analysis of Effect of Substrate Surface Roughness on Liquid Droplet Impact and Flattening Process

Z.G. Feng, M. Domaszewski, G. Montavon, and C. Coddet

(Submitted 28 August 2000; in revised form 19 December 2000)

A computational program using the finite element method has been developed to simulate the impact and flattening of a metal droplet impacting onto a solid surface with different surface roughness occurring in the plasma thermal spray. The model is based on Navier-Stokes equations combining with friction conditions on the substrate surface to simulate the effect of substrate surface roughness on the flattening process of the droplet. In this study, a moving free surface model based on the Lagrangian method with an automatic adaptive remeshing technique has been developed to handle the large deformation of droplets and to ensure the computational accuracy of the numerical results. The numerical results show that the substrate surface roughness has a significant influence on the spreading velocity, flattening ratio, flattening time, splat size, and shape. The spreading process of a droplet is governed not only by the inertia and viscous forces, but also by the frictional resistance of the substrate surface.

Keywords free surface, impact, Lagrangian finite element method, remeshing

1. Introduction

During the plasma thermal-spraying process, metallic or ceramic particles of micron size order are made molten, accelerated, and injected onto a substrate or onto previously deposited layers to produce a strong mechanical and/or anticorrosive coating. The building process of a coating includes the impact, the spreading, and the solidification of individual lamellae. These physical phenomena are complex and occur very rapidly on a microscopic scale. It is difficult to investigate them with experimental methods.

The impact problem of the liquid droplet is very complicated by accompanying the rapid motion of free surface liquid/air and the interface of liquid/solid with the large deformation of liquid droplet as well as the simultaneous heat transfer from molten particle to the substrate. There are the significant difficulties in determining an appropriate numerical model with which to treat these phenomena all together, especially in dealing with the free surface problem. The predominant numerical methods dealing with the free surface problem can be classified into the following two categories in the literature: surface-tracking methods and volume-tracking methods. The surface-tracking methods can give a more accurate description of the free surface. But the main problem is that the element distortion is severe, and it is difficult to handle the large deformations if the remeshing technique has not been used. On the contrary, the volume-tracking methods can handle complicated liquid regions more easily. But the volume-tracking methods cause significant inaccuracy in the treatment of boundary conditions and the orientation of the free surface.[1]

In the literature, the most of the numerical models[2-7] use the volume-tracking methods (e.g., marker-and-cell (MAC) method[8] and volume of fluid (VOF) method[9]). Since the spreading process involves large deformations (for example, the splat thickness is commonly 20 times smaller than the initial droplet diameter) as well as the severe nonuniformity across the splat thickness occurring during spreading, the employment of a fixed grid may be questionable.[10-12] In addition, early investigations emphasize mainly the flattening and heat transfer process under the different impact and material parameters, whereas the effect of surface roughness on the flattening process has been ignored.

The objective of this article is to develop a Lagrangian finite element model combined with an automatic remeshing technique for simulating the impact and spreading process of liquid metal droplets during the plasma thermal spray process. The effect of substrate surface roughness has been investigated by introducing a friction condition on the substrate surface. The computational program is developed by the authors using C++ language. The time-dependent and nonlinear Navier-Stokes equations in primitive variables are solved by using Euler implicit and Newton-Raphson methods.[13]

2. Mathematical and Numerical Models

The model is formulated to simulate the impact of a liquid droplet on a substrate, and the computations start at the instant that the droplet comes into contact with the substrate and proceeds until the droplet comes to rest after the spreading process is completed. Figure 1 shows the schematic of the problem, an

Z.G. Feng, Ansoft Corporation, 4675 Stevens Creek Blvd, Santa Clara, CA 95051; **M. Domaszewski,** Département Génie Mécanique, Université de Technologie de Belfort-Montbéliard, 90010 Belfort Cedex, France; and **G. Montavon** and **C. Coddet,** LERMPS, Université de Technologie de Belfort-Montbéliard, 90010 Belfort Cedex, France. Contact e-mail: fengzhigang@hotmail.com.

initially spherical droplet (diameter d_0) with initial velocity V_0 that impacts onto a solid surface. The coordinate system is represented by the radial and axial coordinates (r, z). The primitive variables are radial velocity u, axial velocity v, and pressure p. The impact and spreading process time is denoted by t.

The motion of a liquid is governed by the laws of the conservation of mass and momentum. These equations consist in a set of coupled partial differential equations in terms of velocity and pressure. The mathematical model developed in this article is based on the following assumptions: laminar, viscous and incompressible fluid; an axisymmetric system of coordinates; and vertical impingement on the substrate. The presence of zeros on the diagonals corresponding to the pressure variables in the mass conservation equation causes difficulties in the resolution of linear algebraic equations. To solve the problem numerically, the artificial compressibility method[14] was used and the governing equations became as follows:

Nomenclature

c	Sound velocity, $m.s^{-1}$
d_0	Droplet initial diameter, m
C	Convection matrix
D	Splat diameter, m
E_t	kinetic energy, Nm
E_k	spreading kinetic energy, Nm
E_v	viscous dissipation energy, Nm
E_f	frictional dissipation energy, Nm
E_s	Surface energy, Nm
F_s	Surface force vector
F_t	Friction force vector
F_r	Froude number, $V_0.g^{-1}d_0^{-1}$
g	Gravity acceleration, $m.s^{-2}$
K	Viscous matrix
M	Mass matrix
M_a	Mach number, $V_0.c^{-1}$
n_i	Normal component
p	Pressure, $N.m^{-2}$
p_0	Ambient pressure, $N.m^{-2}$
r	Radial coordinate, m
R_e	Reynolds number, $\rho d_0 V_0.\mu^{-1}$
R_s	Curvature radius
t	Time, s
Δt	Computational Time step
U	Variable vectors, (u, v, p)
u	Radial velocity, $m.s^{-1}$
v	Axial velocity, $m.s^{-1}$
V_0	Initial velocity of impact, $m.s^{-1}$
W_e	Weber number, $\rho d_0 V_0^2.\gamma^{-1}$
$\bar{x}$	Dimensionless variable
z	Axial coordinate, m
ξ	flattening ratio, $D.d_0^{-1}$
ρ	Density, $kg.m^{-3}$
μ	Dynamic viscosity, $kg.m^{-1}.s^{-1}$
λ	Friction factor
γ	Surface tension coefficient,
σ_{rr}	Radial surface tension, $N.m^{-2}$
σ_{zz}	Axial surface tension, $N.m^{-2}$
ψ	Surface curvature

$$M_a^2 \frac{\partial \bar{p}}{\partial \bar{t}} + \frac{\partial \bar{u}}{\partial \bar{r}} + \frac{\partial \bar{v}}{\partial \bar{z}} + \frac{\bar{u}}{\bar{r}} = 0 \quad \text{(Eq 1)}$$

$$\frac{\partial \bar{u}}{\partial \bar{t}} + \bar{u}\frac{\partial \bar{u}}{\partial \bar{r}} + \bar{v}\frac{\partial \bar{u}}{\partial \bar{z}} = -\frac{\partial \bar{p}}{\partial \bar{r}} + \frac{1}{R_e}\left(\frac{\partial^2 \bar{u}}{\partial \bar{z}^2} + \frac{\partial^2 \bar{u}}{\partial \bar{r}^2} + \frac{1}{\bar{r}}\frac{\partial \bar{u}}{\partial \bar{r}} - \frac{\bar{u}}{\bar{r}^2}\right) + \frac{1}{F_r} e_g \quad \text{(Eq 2)}$$

$$\frac{\partial \bar{v}}{\partial \bar{t}} + \bar{u}\frac{\partial \bar{v}}{\partial \bar{r}} = \bar{v}\frac{\partial \bar{v}}{\partial \bar{z}} = -\frac{\partial \bar{p}}{\partial \bar{z}} + \frac{1}{R_e}\left(\frac{\partial^2 \bar{v}}{\partial \bar{z}^2} + \frac{\partial^2 \bar{v}}{\partial \bar{r}^2} + \frac{1}{\bar{r}}\frac{\partial \bar{v}}{\partial \bar{r}}\right) + \frac{1}{F_r} e_g \quad \text{(Eq 3)}$$

where, e_g represents the unit vector along the gravitational direction and M_a, R_e, and F_r are, respectively, Mach, Reynolds, and Froude numbers, which are defined as follows:

$$M_a = \frac{V_0}{c} \quad R_e = \frac{\rho V_0 d_0}{\mu} \quad F_r = \frac{V_0^2}{g\, d_0} \quad \text{(Eq 4)}$$

where c is the speed of sound in the fluid medium, ρ is the density, μ is the dynamic viscosity of the fluid, g is the gravitational acceleration, and d_0, V_0 are the initial diameter and the initial impact velocity, respectively.

In the above dimensionless axisymmetric conservation (Eq 1-3), the nondimensionalizations for the coordinates (r, z), the time (t), and the variables of velocities and pressure (u, v, and p) were carried out according to the following definitions.

$$\bar{r} = \frac{r}{d_0} \quad \bar{z} = \frac{z}{d_0} \quad \bar{t} = \frac{t\, V_0}{d_0}$$
$$\bar{u} = \frac{u}{V_0} \quad \bar{v} = \frac{v}{V_0} \quad \bar{p} = \frac{p_0}{\rho V_0^2} \quad \text{(Eq 5)}$$

For this study, the boundary conditions are presented in Fig. 2. The analysis is performed on a half model because of axisymmetry. The computational domain is formed by the free surface S_1, axisymmetric axis S_2, and the droplet-substrate interface S_3.

At the free surface, the physical condition that there is no mass flux across the free surface requires that the surface must move and deform on a material surface, which yields to the following cinematic condition.

$$\frac{Dx}{Dt} = u \quad \text{(Eq 6)}$$

where x and u are the displacement and velocity vectors.

The conservation of linear momentum across the free surface gives rise to the dynamic condition for the stress field.

$$\sigma_{ij}\, n_j = (\gamma\psi + p_0) n_i \quad \text{(Eq 7)}$$

where σ_{ij} are the components of stress tensor, n_i is the component of the outer unit normal to the free surface, γ is the surface tension coefficient of the fluid, p_0 is the ambient pressure, and ψ is the mean surface curvature, which is the reciprocal of the curvature radius R_s. So, there are stress components at the free surface.

$$\sigma_{rr} = \left(\gamma\frac{1}{R_s} + p_0\right) n_r \quad \sigma_{zz} = \left(\gamma\frac{1}{R_s} + p_0\right) n_z \quad \text{(Eq 8)}$$

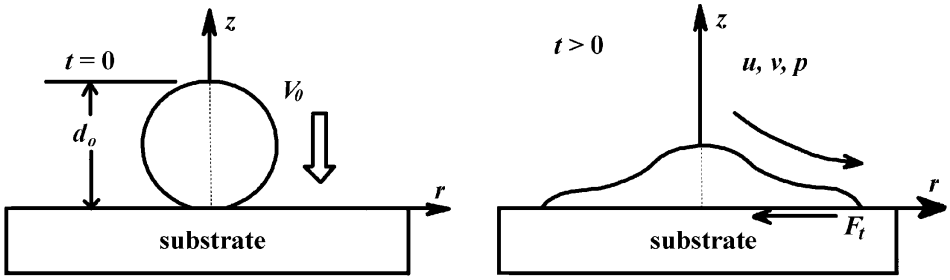

Fig. 1 Schematic of the problem of interest

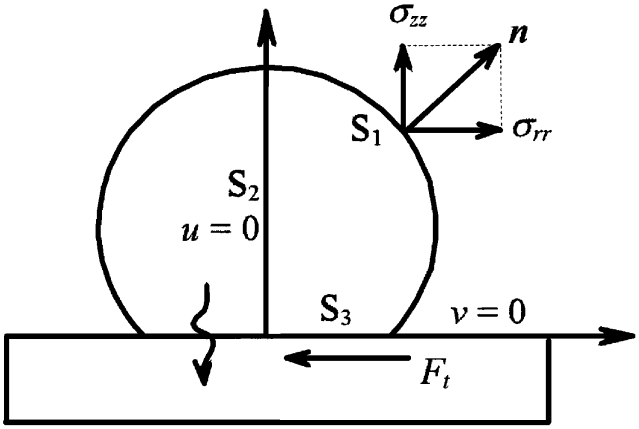

Fig. 2 Boundary conditions used in this study

The dimensionless quantities for the surface tension (σ_{rr}, σ_{zz}) and the curvature radius R_s, were carried out according to the following definitions.

$$\bar{\sigma}_{zz} = \frac{\sigma_{zz}}{\rho V_0^2} \quad \bar{\sigma}_{rr} = \frac{\sigma_{rr}}{\rho V_0^2} \quad \bar{R}_s = \frac{R_s}{d_0} \tag{Eq 9}$$

Substituting the above equation into Eq 8, the dimensionless surface tensions are obtained as follows.

$$\begin{aligned} \bar{\sigma}_{zz} &= \frac{\gamma}{\rho V_0^2 d_0 \bar{R}_s} n_z = \frac{1}{W_e} \frac{1}{\bar{R}_s} n_z \\ \bar{\sigma}_{rr} &= \frac{\gamma}{\rho V_0^2 d_0 \bar{R}_s} n_r = \frac{1}{W_e} \frac{1}{\bar{R}_s} n_r \end{aligned} \tag{Eq 10}$$

where, the Weber number W_e and the curvature radius are defined as follows.

$$W_e = \frac{p V_0^2 d_0}{\gamma} \quad \frac{1}{\bar{R}_s} = d_0 \left(\frac{1}{R_1} + \frac{1}{R_2} \right) \tag{Eq 11}$$

with R_1 and R_2 being the principal radii of curvature of the surface, which are defined as follows.[15]

$$R_1 = \frac{[1 + (d\bar{r}/d\bar{z})^2]^{1.5}}{d^2\bar{r}/d\bar{z}^2}, \quad R_2 = \bar{r}\left[1 + \left(\frac{d\bar{r}}{d\bar{z}} \right)^2 \right]^{0.5} \tag{Eq 12}$$

Concerning the boundary condition at the droplet-substrate interface, generally, the adherence or smooth condition (Fig. 3a and c) was used in almost all research[2-7] about the simulatio n of the impact of a liquid droplet onto a solid substrate. But these two types of boundary conditions do not represent the real situation when a droplet impinges onto a solid substrate, because the experimental research has demonstrated the large influence of substrate roughness on the spreading process of a liquid droplet.[16] In this study, the friction force boundary condition (Fig. 3b) is utilized to study the effect of substrate roughness on the spreading process. According to the expression developed in a previous article,[17] the friction force F_t depends on the fluid density, the radial velocity at the droplet-substrate interface, and the substrate roughness, which can be described as follows.

$$F_t = -\lambda \rho |\bar{u}| \bar{u} \tag{Eq 13}$$

where λ is the friction factor in an experimental coefficient, which depends on the state of the substrate surface, ρ is the droplet density, and u is the tangent velocity on the droplet-substrate interface, and the negative sign means that the friction force F_t has the opposite direction to the tangent velocity.

Using the Rayleigh-Ritz-Galerkin method, the finite element model of the governing Eq 1 to 3 are given by:

$$M\dot{U} + C(u,v)U + KU = F_s + F_t \tag{Eq 14}$$

where U is variable vectors (p, u, and v), M is the mass matrix, $C(u,v)$ is the convection matrix, which is the function of velocities, K is the viscous matrix, F_s is the surface force vector, and F_t is the friction force vector.

Figure 4 shows the element types used in this study. The triangle element is used to mesh the droplet domains. On the droplet-substrate interface, the two-node linear element is used to represent the substrate surface for simulation of the effect of substrate roughness on the fluid flow.

The Lagrangian formulation is applied to track accurately the moving of the free surface. The finite element mesh is attached to the materials. This implies that the motion of the material is inferred from the motion of the mesh after calculation in each step. In order to control the severe distortion of the computational mesh inherent in the Lagrangian finite element approach, it is necessary to adopt a remeshing strategy when the monitored element shapes exceed a prescribed limit. This criterion is expressed as follows:

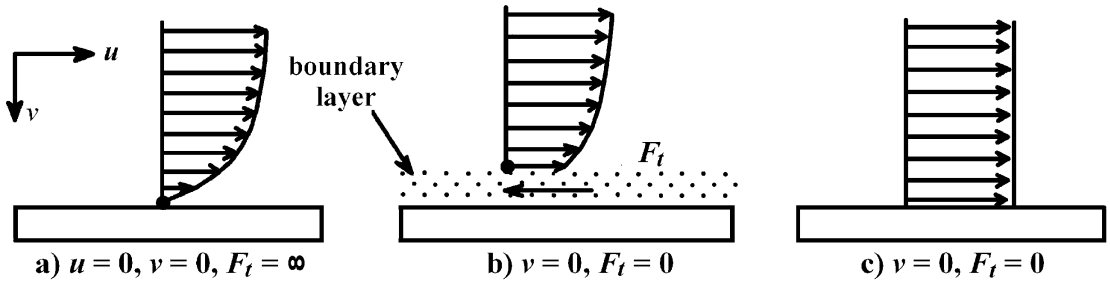

Fig. 3 Boundary conditions at the solid wall surface

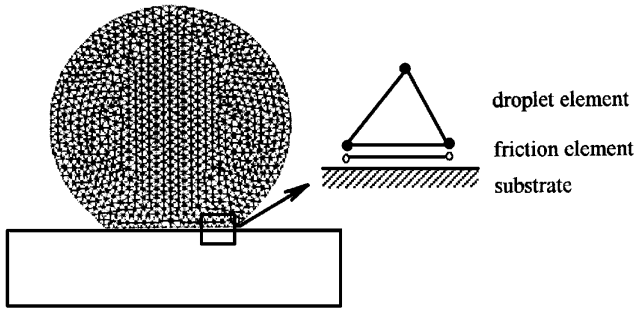

Fig. 4 Element types used in this study

$$\frac{L_{\max}}{L_{\min}} \geq 4.5 \qquad \text{(Eq 15)}$$

where L_{max} and L_{min} represent the element longest and the shortest side, respectively. The procedure of the automatic remeshing technique used in this study consists of the following steps.

1) Perform a Lagrangian step: according to the solution of the velocity field, the new position of the old computational mesh can be obtained by $X^{n+1} = X^n + \Delta t \cdot u^{n+1}$;
2) Control the deformation of the element: a prescribed limit is imposed to check the shape of elements near the substrate where the largest deformation occurs;
3) Define the boundary nodes: according to the results of the Lagrangian step, define the boundary nodes and smooth boundary nodes uniformly by interpolation;
4) Generate a new mesh: with the knowledge of boundary nodes, the new mesh for the interior domain is created by using the Delaunay algorithm[18,19];
5) Transfer the values: in the program, two cycles are set up, one for the node number of new mesh and another for the element number of the old mesh. The interpolation is performed when a node in the new mesh is placed in an old element.

3. Numerical Results and Discussion

For the purpose of this study, a fully molten pure aluminum droplet impacting onto a rigid steel substrate was considered. The simulation parameters and the physical properties of the spray material used in the numerical computation are given in Table 1.

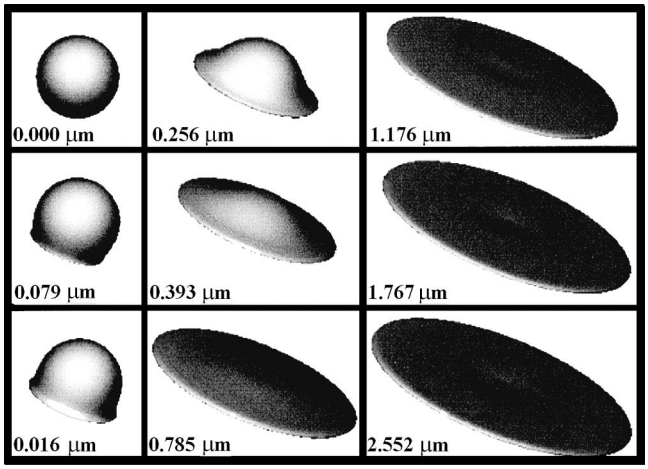

Fig. 5 Spreading process of a liquid droplet onto fine substrate surface

Table 1 Simulation Parameters and the Physical Properties

Material	Aluminum Droplet	Steel Substrate	Units
Density	2.38×10^3	7.832 1 10^3	kg/m^3
Viscosity	2.9×10^{-3}		Pa
Geometric size	diameter: 50	thickness: 25	μm
Initial velocity	100.0	0.0	m/s
Roughness factorλ	2.5×10^{-3}, 0.25, 040		

Early computations showed that roughness factors lower than 2.5×10^{-3} and higher than 4.0 did not significantly modify the flattening processes in the case of the impact of aluminum droplet impacting onto a rigid steel substrate. In the following computations, these values were considered for the roughness factors: 2.5×10^{-3}, 0.25, and 4.0, respectively, corresponding to smooth (i.e., polished), fine (i.e., machined), and coarse (i.e., grit blasted) substrates surfaces.

Figure 5 shows the three-dimensional images of the flattening process of a liquid droplet on a fine substrate surface. At the beginning of the impact, the liquid droplet spreads rapidly at the droplet-substrate interface. With increasing time, the splat height decreases and its diameter increases. Figure 6 shows the deformation of the mesh during the impact process. It is noted that the mesh is always uniform in the computation due to an automatic remeshing technique.

Table 2 shows the final flattening ratio, splat size, and maxi-

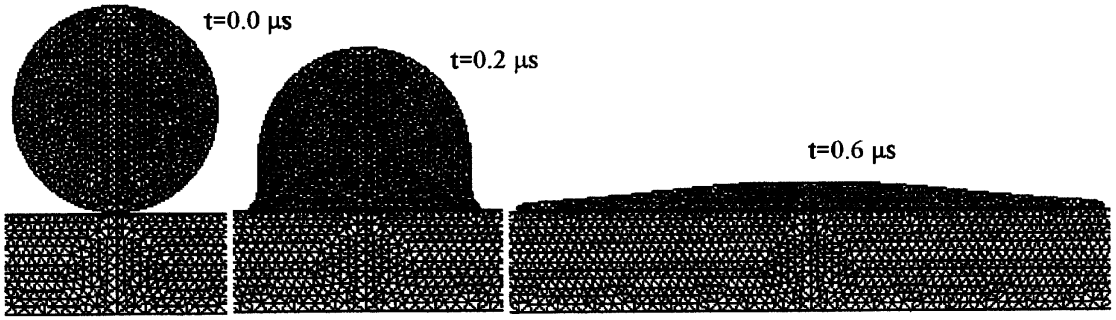

Fig. 6 Deformed mesh at different time steps

Table 2 The Final Sizes of Splat and the Total Flattening Time

Parameters	Smooth Surface	Fine Surface	Coarse Surface
Flattening ratio	6.52	3.91	2.57
Flattening time, μs	3.74	2.93	2.20
Splat diameter, μm	317.01	178.6	125.5
Splat height, μm	1.243	2.615	5.241

Table 3 Analytical Solutions of Flattening Ration ($\varepsilon = a\,(R_e)^b$, $R_e = 4103.45$)

Authors	Coefficient *a*	Coefficient *b*	ε
Madejski [20]	1.2941	0.2	6.83
Liu et al. [21]	1.04	0.2	5.49
Trapaga et al. [22]	1.0	0.2	5.28
Fantassi et al. [23]	0.83	0.2	4.38
Fukanuma and Ohmori [24]	1.06	0.1667	4.24
Jones [25]	1.16	0.125	3.28

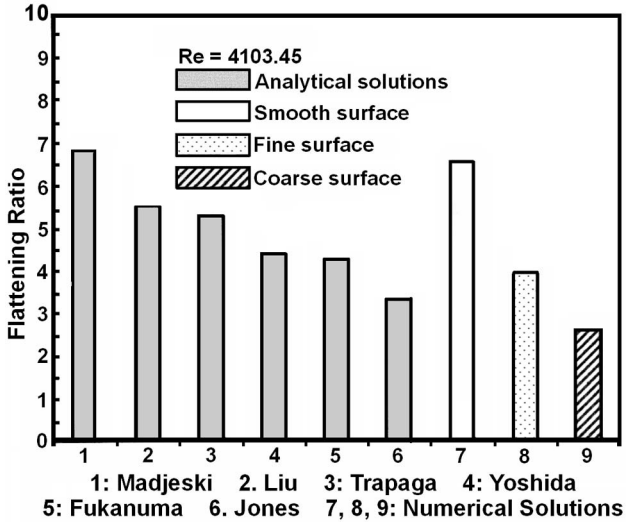

Fig. 7 Comparison between the analytical and numerical solutions for the flattening ratio

mum spreading time of a droplet in three cases where it impacts onto three kinds of substrate surfaces (smooth, fine, and coarse). It is evident that the smoother the surface, the larger the splat surface and the longer the flattening time. With the analytical methods, several authors[20-25] have proposed a similar formula about the relationships between the flattening ratio (ξ) and the Reynolds number (R_e) as follows:

$$\xi = a(R_e)^b \qquad \text{(Eq 16)}$$

With the parameters used in this study, the Reynolds number is obtained

$$R_e = \rho\, d_0 V_0 \mu = 4103.45$$

Substituting this value into Eq 16, the analytical solutions about the flattening ratio are shown in Table 3. It can be found that the numerical and analytical results are situated in the same order. In the case of a droplet impacting onto a coarse surface, the analytical solutions are much higher than the numerical results because of the influence of substrate surface roughness, as shown in Fig. 7.

Figure 8 shows the radial velocity of the contact point of free surface substrate at every computation time step. The highest

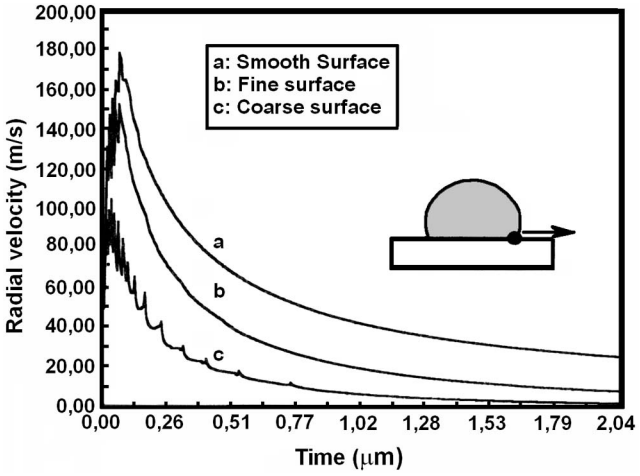

Fig. 8 Radial velocity evolution vs time

radial spreading velocity can arrive at a speed that is 1.8 times that of impact velocity, which is close to the results (two times that of impact velocity) of Liu et al.[21] in which the surface friction was ignored.

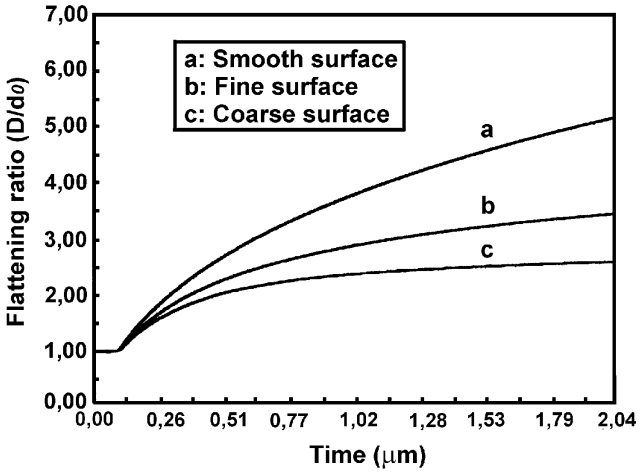

Fig. 9 Flattening ratio of droplet evolution vs time

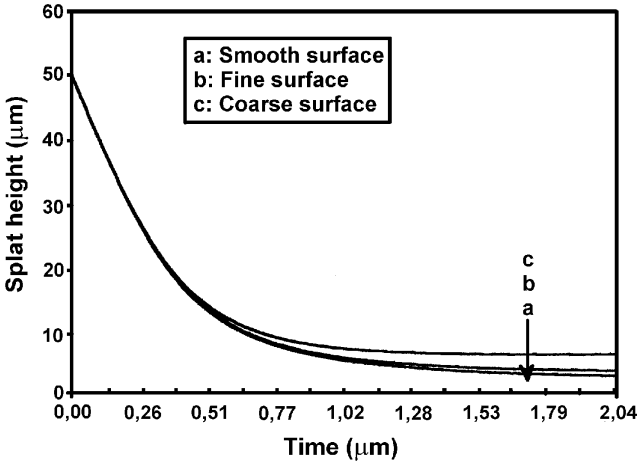

Fig. 10 Splat height evolution vs time

Figures 9 and 10 show the influences of surface roughness on the evolution of the flattening ratio of the liquid droplet and the splat height. The numerical results indicate that the substrate roughness has significant influence not only on the spreading velocity, degree of flattening, flattening time of the liquid droplet, and the splat size, but also on the splat shape. The surface roughness changes the contact angle during the spreading process of the droplet. As shown in Fig. 11, the smoother the surface, the larger the contact angle.

The effect of roughness on the spreading process of a liquid droplet (i.e., degree of flattening, flattening time, velocity distribution, and splat size and shape) can be explained by its effect on the spreading kinetic energy. The spread of a liquid droplet is driven by the kinetic energy prior to the impact. During the spreading process, the conservation of mechanical energy is defined as follows:

$$E_t = E_k + E_v + E_f + E_s \quad \text{(Eq 17)}$$

where, E_t is the sum of kinetic energy prior to the impact, E_k is the spreading kinetic energy of the liquid droplet, E_v is the viscous dissipation energy, E_f is the frictional dissipation energy, and E_s is the surface energy.

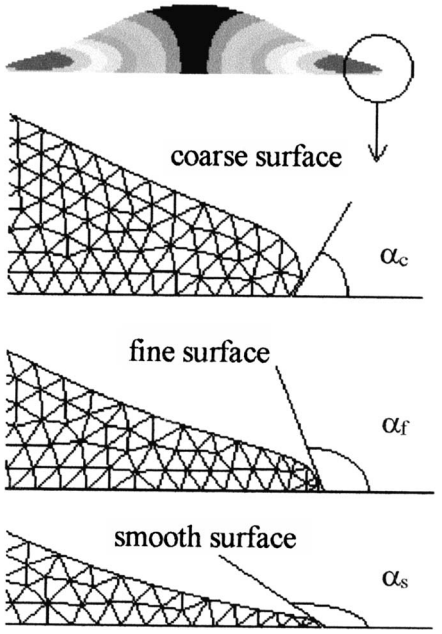

Fig. 11 Influences of surface roughness on contact angle (spreading time, 0.393 μs)

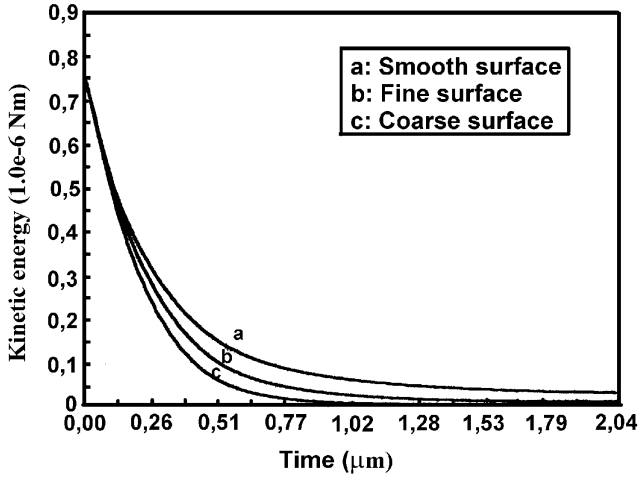

Fig. 12 Kinetic energy evolution vs time

It is clear that the frictional dissipation energy increases with the surface roughness. Hence, this results in the decrease of the spreading kinetic energy E_k (Fig. 12). As a result, the spreading velocity, the degree of flattening, and the flattening time decrease with increasing surface roughness. These numerical results correspond to the experimental results.[16,26-28]

4. Conclusion

A Lagrangian finite element model coupled with an automatic remeshing technique was developed to study the effect of

substrate surface roughness on liquid droplet impact and the flattening process. The numerical results show that the spreading process of a droplet is governed not only by inertia and viscous forces but also by the frictional resistance of the substrate surface. The substrate surface roughness has a significant influence on the spreading velocity, flattening ratio, flattening time, splat size, and splat shape. With the increase of surface roughness, the spreading velocity, the flattening ratio, the flattening time, and the contact angle between the splat and the substrate surface decrease.

Acknowledgments

This work was supported by the Scientific Council of the Université de Technologie de Belfort-Montbéliard, Belfort, France, under grant program No. 9526.

References

1. F. Mashayer and N. Ashgriz: "A Hybrid Finite Element Volume-Of-Fluid Method for Simulating Free Surface Flows and Interfaces," *Int. J. Numerical Methods Fluids*, 1995, *20*, pp. 1363-80.
2. F.H. Harlow and J.E. Welch: "Numerical Calculation of Time-Dependent Viscous Incompressible Flow of Fluid with Free Surface," *Phys. Fluids*, 1995, *8*, pp. 2182-94.
3. Z. Trapaga and J. Szekely: "Mathematical Modeling of the Isothermal Impingement of Liquid Droplets in Spraying Processes," *Metal. Trans. B*, 1991, *22*, pp. 901-14.
4. H. Liu, E.J. Lavernia, and R.H. Rangel: "Numerical Simulation of Impingement of Molten Ti, Ni and W Droplets on a Flat Substrate, *J. Thermal Spray Technol.*, 1993, *2*(4), pp. 369-78.
5. T. Watanabe, M. Yao, J. Senda, and H. Fujimoto: "Deformation and Solidification of Droplet on a Cold Substrate," *Chem. Eng. Sci.*, 1992, *47*, pp. 3059-65.
6. M. Pasandideh-Fard, R. Bhola, S. Chandra, and J. Mostaghimi: "Deposition of Tin Droplet on a Steel Plate Simulations and Experiments," *Int. J. Heat Mass Transfer*, 1998, *41*, pp. 2929-45.
7. C.-J. Li and J.-L. Li: "Transient Droplet/Substrate Contact Pressure During Droplet Flattening on Flat Substrate in Plasma Spraying," in *Proc. 1st Int. Thermal Spray Conf.*, C. C. Berndt, ed., 2000, pp. 777-82.
8. E.A.J. Fletcher: *Computational Fluid Dynamics*, Vol. II., Springer, Berlin, Germany, 1988, pp. 333-45.
9. C.W. Hirt and B.D. Nichols: "Volume of Fluid (VOF) Method for the Dynamics of Free Boundaries," *J. Comput. Phys.*, 1981, *39*, pp. 201-11.
10. J. Fukai, Y. Shiiba, T. Yamamoto, O. Miyatake, D. Poulikakos, C. M. Megaridis, and Z. Zhao: "Wetting Effects on the Spreading of a Liquid Droplet Colliding with a Flat Surface: Experiment and Modeling," *Phys. Fluids*, 1995, *7*, pp. 236-47.
11. Z. Zhao and D. Poulikakos: "Heat Transfer and Fluid Dynamics During the Collision of a Liquid Droplet on a Substrate: I. Modeling," *Int. J. Heat Mass Transfer*, 1996, *13*, pp. 2771-89.
12. Z.G. Feng: "Modélisation Numérique de L'impact d'une Particule Fondue sur une Surface Solide avec Transfert Thermique," Ph.D. Thesis, Université de Technologie de Belfort-Montbéliard, Belfort, France, 1996.
13. W.H. Press, S.A. Teukolsky, W.T. Vetterling, and B.P. Flannery: *Numerical Recipes in C, The Art of Scientific Computing*, 2nd ed., Cambridge University Press, Cambridge, UK, 1992, pp. 362-69.
14. O.C. Zienkiewitz and R.L. Taylor: The Finite Element Method, 4th ed. Vol 2, McGraw-Hill, London, UK, 1991, pp. 513-14.
15. K.J. Bathe, H. Zhang, and M.H. Wang: "Finite Element Analysis of Incompressible and Compressible Fluid Flows with Free Surfaces and Structural Interactions," *Comput. Struct.*, 1995, *56*(2/3), pp. 193-213.
16. C. Moreau, P. Gougeon, and M. Lamontagne: "Influence of Substrate Preparation on the Flattening and Cooling of Plasma-Sprayed Particles," *J. Thermal Spray Technol.*, 1995, *4*(1), pp. 25-33.
17. Z.G. Feng, Z.Q. Feng, M. Domaszewski, and G. Montavon: "Lagrangian method and remeshing technique for modeling of spreading of liquid particle during plasma spray process," *IDMME'98—2nd International Conference on Integrated Design and Manufacturing in Mechanical Engineering*, Compiègne, France, May 27-29, 1998, *1*, pp. 175-82.
18. M. Berg, M. Kreveki, M. Overmars, and O. Schwarzkopf: *Computational Geometry: Algorithms and Applications*, Springer-Verlag, Berlin, Germany, 1997, pp. 126-58.
19. E.F. D'Azevedo: "On Adaptive Mesh Generation in Two-Dimensions," *Proc. 8th International Meshing Roundtable*, South Lake Tahoe, CA, October 1999, pp. 236-48.
20. J. Madejski: "Solidification of Droplet on a Cold Surface," *J. Heat Mass Transfer*, 1976, *19*, pp. 1009-13.
21. H. Liu, E.J. Lavernia, R.H. Rangel, E. Muehlberger, and A. Sickinger: "Deformation and Interaction Behavior of Molten Droplets Impinging on a Flat Substrate in Plasma Spray Process," *Proc. 1993 National Thermal Spray Conf.*, Anaheim, CA, June 7-11, 1993, pp. 457-62.
22. G. Trapaga E.F. Matthys, J.J. Valencia, and J. Szekely: "Fluid Flow, Heat Transfer, and Solidification of Molten Metal Droplets Impinging on Substrates: Comparison of Numerical and Experimental Results," *Metall. Trans. B*, 1992, *23*, pp. 701-18.
23. S. Fantassi , M. Vardelle, A. Vardelle, and P. Fauchais: "Influence of the Velocity of Plasma Sprayed Particles on the Splat Formation," in *Thermal Spray Coatings: Research, Design and Applications*, C.C. Berndt and T.F. Bernecki, ed., ASM International, Materials Park, OH, 1993, pp. 1-6.
24. H. Fukanuma and A. Ohmori: *Proc. 7th NTSC*, Boston, MA, June 1994, pp. 563-68.
25. H. Jones: "Cooling, Freezing and Surface Impact of Droplets Formed by Rotary Atomization," *J. Phys. D: Appl. Phys.*, 1971, *4*, pp. 1657-60.
26. S. Sampath, X. Y. Jiang, J. Matejicek, A. C. Leger, and A. Vardelle: "Substrate Temperature Effects on Splat Formation, Microstructure Development and Properties of Plasma Sprayed Coatings: Part I. Case Study For Partially Stabilized Zirconia," *Mater. Sci. Eng. A*, 1999, *A272*, pp. 181-92.
27. P. Fauchais and A. Vardelle: "Splat Formation and Cooling of Plasma Sprayed Zirconia," *Thin Solid Films*, 1997, *305*, pp. 35-47.
28. Y.P. Wan, H. Zhang, X.Y. Jiang, S. Sampath, and V. Prasad: "Role of Solidification, Substrate Temperature and Reynolds Number on Droplet Spreading in Thermal Spray Deposition: Measurements and Modeling," *J. Heat Transfer*, 2000, in press.